

Regular Paper

## Segmentation of CT Brain Images Using Unsupervised Clusterings

Tong Hau Lee<sup>\*1</sup>, Mohammad Faizal Ahmad Fauzi<sup>\*2</sup> and Ryoichi Komiya<sup>\*1</sup>

\*1 Faculty of Information Technology, Multimedia University, Jalan Multimedia, 63100 Cyberjaya, Selangor, Malaysia. E-mail: hltong@mmu.edu.my

\*2 Faculty of Engineering, Multimedia University, Jalan Multimedia, 63100 Cyberjaya, Selangor, Malaysia.

Received 23 May 2008  
Revised 3 November 2008

**Abstract** In this paper, we present non-identical unsupervised clustering techniques for the segmentation of CT brain images. Prior to segmentation, we enhance the visualization of the original image. Generally, for the presence of abnormal regions in the brain images, we partition them into 3 segments, which are the abnormal regions itself, the cerebrospinal fluid (CSF) and the brain matter. However, for the absence of abnormal regions in the brain images, the final segmented regions will consist of CSF and brain matter only. Therefore, our system is divided into two stages of clustering. The initial clustering technique is for the detection of the abnormal regions. The later clustering technique is for the segmentation of the CSF and brain matter. The system has been tested with a number of real CT head images and has achieved satisfactory results.

**Keywords** Medical images, Visualization enhancement, Image segmentation, Computed tomography, Unsupervised clustering.

### 1. Introduction

Computed tomography (CT) images can be distinguished for different tissues according to their different gray levels. The images, if processed appropriately can offer a wealth of information which is significant to assist doctors in medical diagnosis.

Image segmentation is the process of partitioning a digital image into sets of pixels. Accurate, fast and reproducible image segmentation technique is required in various applications. The results of the segmentation are significant for classification and analysis purposes. CT scans of internal organs, bone and soft tissue furnish greater clearness than conventional x-ray. On the other hand, Magnetic Resonance Imaging (MRI) scan produces clearer images and a greater resolution compared with CT scan with lower resolution which may cause some small lesions go undetected.

The limitations for CT scanning of head images are due to partial volume effects which affect the edges, produce low brain tissue contrast and yield different objects within the same range of intensity. All these limitations have made the segmentation more difficult. Therefore, the challenges for automatic segmentation of the CT head images have raised many different approaches. The segmentation techniques developed so far include statistical pattern recognition techniques (e.g., Nathalie et al, 2007; Y. Zhang et al, 2001), morphological processing with thresholding (e.g., K. H. Hohne et al, 1992; Lemieux et al, 1999), clustering algorithm (e.g., Qingmao et al, 2005; N. A. Mohamed et al, 1999) and active contour (e.g., Albert et al, 2006; Ruzica et al, 2000). Wei et al, 2007 introduced the effective particle swarm optimization (PSO) algorithm to segment the brain images into CSF and suspicious abnormal regions but without the annotation of the abnormal regions.

Dubravko et al, 1997 and Matesin et al, 2001 from the segmentation results apply the rule-based approach to label the abnormal regions such as calcification, hemorrhage and stroke lesion.

In our work, first we attempt to detect and separate the abnormal regions. Then the remaining regions in the image will be segmented into 2 clusters which are CSF and brain matter. The originality of this paper is to present a unique approach for the segmentation of CT head images by applying and combining existing algorithms in different stages and ways. The main contribution of this work is that the obtained results from the image segmentation will be employed to create an automatic image retrieval system for collaborating hospital.

## 2. System Overview

Most segmentation techniques offer just one level of segmentation to segment all the regions. However, in our approach we adopt the different methods to segment different brain parts. This is due to the some abnormal regions which are too small to form a cluster themselves. The flowchart of the system is shown as in Fig. 1.

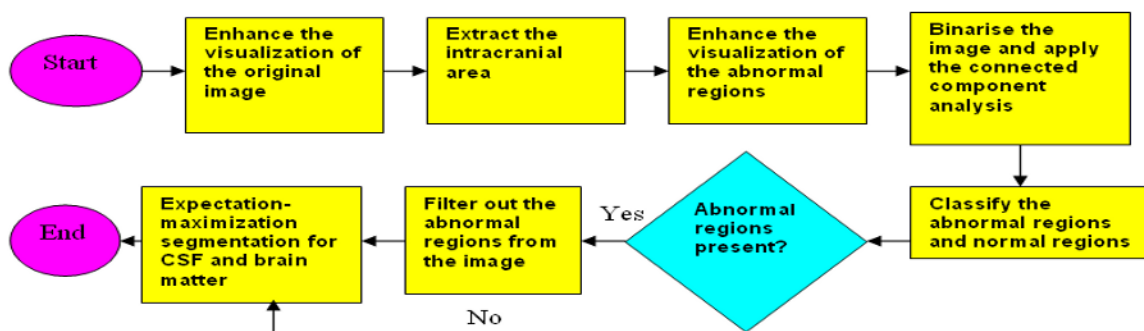


Fig. 1. Flow chart for the system for segmentation of CT brain images.

From Figure 1, the initial step is to apply the contrast stretching in order to boost the visualization of the original low contrast image. After improvement of the visualization of the image, intracranial area is extracted from the contrast stretched image. In order to detect the abnormal regions, we adopt the contrast enhancement for the second time to improve the visualization of the abnormal regions.

For the binarization of the image, we experiment on four methods which are k-means clustering, fuzzy c-means (FCM) clustering, expectation-maximization(EM) clustering and Otsu threshold. From our observation, we discovered that only two methods which are k-means and FCM clustering can be adopted to identify the potential abnormal regions. After binarization, we apply the connected component analysis and extract all the features from each connected component. Once all features are extracted, we classify all regions according to normal and abnormal regions by using the decision tree. If the abnormal regions are present, we filter out all the abnormal regions before moving on to the next stage. Eventually we apply the EM algorithm to segment the brain CSF and brain matter area.

## 3. Implementation Process

### 3.1 Visualization Enhancement of the Original Image

The low distribution of the gray levels of the original image reduces the contrast of the image. Therefore contrast stretching is employed to increase the dynamic range of the gray levels in the images. The low limit and upper limit for linear contrast stretching are automatically determined from the histogram. Firstly, we construct the histogram of the original image as depicted in Fig. 2(a). From the constructed histogram, it exhibits several peaks. Basically the left peak and the rightmost peak are contributed by the background pixels and the soft tissues respectively. Only the rightmost peak contributed by the soft tissues consist of useful information. Therefore, we locate the position of the rightmost peak,  $I_p$ .

In order to obtain a smoother curve, we convolve the histogram in Fig. 2(a) with a vector which each element the value is  $10^{-3}$ . Then, the smoothen curve is transformed into absolute first difference as shown in Fig. 2(b). From the first difference, the closest peak on the left and right of  $I_p$  are auto

determined as the lower limit,  $I_L$  and the upper limit,  $I_U$  respectively for the contrast stretching.  $I_L$  and  $I_U$  will then be considered as the input into the linear contrast stretching algorithm as in equation (1).

$$F(i, j) = I_{\max} \frac{(I(i, j) - I_L)}{(I_U - I_L)} \quad (1)$$

where  $I_{\max}$ ,  $I(i, j)$  and  $F(i, j)$  denote the maximum intensity in the image, original image and enhanced image respectively. After the contrast stretching, the obtained result is shown in the Fig. 3(b). As can be seen, a much better visualization is obtained.

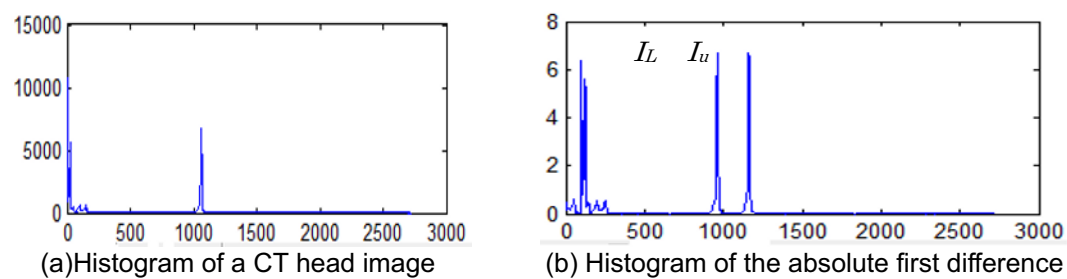


Fig. 2. Example of the histogram.



(a) Original image

(b) Enhanced image

Fig. 3. Example of an image before and after enhancement.

### 3.2 Extraction of the Intracranial Area

In order to extract the intracranial area, we employ thresholding to the enhanced image in Section 3.1. The threshold value,  $T$  is fixed at  $T = I_U + 30$  in order to obtain the skull, as the intensity of the skull is usually exceeded the upper limit of the soft tissues. The thresholded image is shown in Fig. 4(a). Since the skull is always the largest connected component of the brightest regions, we figure out the largest connected component and remove the smaller connected component.

To eliminate the background and skull from the intracranial area, we set the pixel values of the skull and background to zero (black pixel). The intracranial area after stripping of the skull and background is shown in Fig. 4(b).



(a) Thresholded image

(b) Intracranial area

Fig. 4. Example of the intracranial extraction.

### 3.3 Visualization Enhancement of the Abnormal Regions

After intracranial area extraction, the image is further proceeded with the second contrast stretching to improve the visualization of the abnormal regions. In this research works, we consider three types of abnormalities which are calcification, hemorrhage, and lesions. Other bright regions such as sinus, vessel and midline falx are classified as normal regions. The contrast stretching we applied in this section is identical to the contrast stretching in Section 3.1. However, the way of acquiring the lower limit and upper limit now is different from previous section. In order to automatically determine the appropriate lower limit and upper limit for the contrast stretching, we construct the histogram for

the image from Section 3.2. From the constructed histogram, we derive the lower limit,  $I_L$  which is the peak position of the histogram. The upper limit,  $I_U$  is defined as a:

$$I_U = I_L + I_\alpha$$

where  $I_\alpha$  is fixed at 400 found from experimental observation in order to obtain the better result of the enhancement. Besides, this value is set not exceeded 400 to avoid the over-enhancement of the white matter. The over-enhancement will cause the intensity of the white matter of the brain become very similar with the abnormal regions which will result in difficulty for segmentation later. In order to reduce the “salt and pepper” noise, we utilize the median filter. The example of the contrast stretched image is shown in Fig. 5(b).

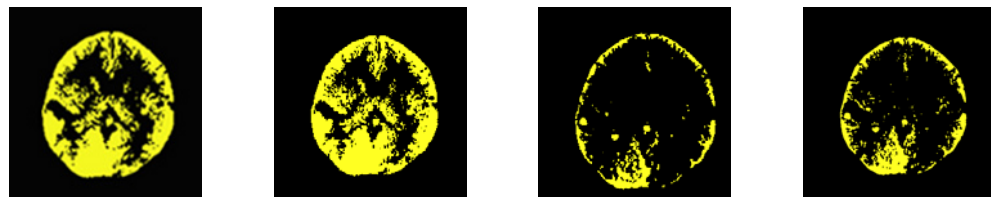


Fig. 5. (a) Original image (b) Image after contrast stretching

### 3.4 Binarization of the Image

In this section, the image is transformed into binary image in order to apply the connected component analysis to detect all the regions in intracranial area. For the binarization of the enhanced image from Section 3.3, we have attempted on four methods which are k-means clustering, FCM clustering, EM segmentation and Otsu threshold. Otsu method finds the optimum threshold that minimizes the within-class variance to turn the graylevel image to a binary image. However, k-means, FCM and EM clustering are unsupervised clustering. For k-means and EM algorithm, each pixel will associate only to one cluster. However, for FCM algorithm each pixel can belong to two or more clusters based on the membership probability. The obtained binarized images for the respective segmentations are shown as in Fig. 6. The original image for Fig. 6 is shown in Fig. 5(a).

From the results, we found that Otsu threshold and EM segmentation are not suitable as the abnormal regions are merged together with the normal region. This makes it impossible to filter out the abnormal region thoroughly. On the contrary, k-means and FCM segmentation produced useful result as the abnormal regions are not merged with the normal regions. This is crucial as the abnormal regions can now be distinguished from the normal regions. The obtained binarized image from k-means and FCM segmentation will be utilized and compared in terms of their classification accuracies for the normal and abnormal regions in the later section.



(a) Otsu threshold (b) EM clustering (c) k-means clustering (d) FCM clustering  
Fig. 6. Binary image by generated by four different methods.

### 3.5 Feature Extraction and Classification of the Normal and Abnormal Regions

Firstly, we extract the features of every connected component obtained in Section 3.4. All the extracted features are depicted in Table 1. After the feature extraction, we have to classify the regions into normal and abnormal region by using the decision tree as shown in Fig. 7. First we distinguish the regions according to whether their adjacent neighbor is a skull or not. In other words, we establish two decision trees respectively for the region adjacent to skull and the region not adjacent to skull.

As shown in the tree diagram, we categorize the area of regions into smaller and larger areas. The reason we divide the area into these two types is because for the smaller areas such as hyperdense lesion, the intensity is lower than larger areas such as calcification and bleeding. Similarly, for the region adjacent to the skull, we form the similar decision tree but with two extra features which are orientation and eccentricity. The orientation and eccentricity are to detect the

midline falx which is the bright area at the top and bottom of the intracranial area so that it won't be misclassified as an abnormal region.

Table 1. Features of the connected component.

| Feature            | Remarks  |
|--------------------|--|
| Area               | The number of pixels in the region of the enhanced image in Section 3.1.   |
| mean               | The average of pixels in the region of the original image in Section 3.1.  |
| Standard deviation | The standard deviation of pixels in the region of the original image in Section 3.1.   |
| Eccentricity       | The value is between 0 and 1. An ellipse whose eccentricity is 0 is actually a circle, while an ellipse whose eccentricity is 1 is a line segment. |
| Orientation        | The angle in degree.   |
| Adjacent neighbor  | Whether skull or not.  |

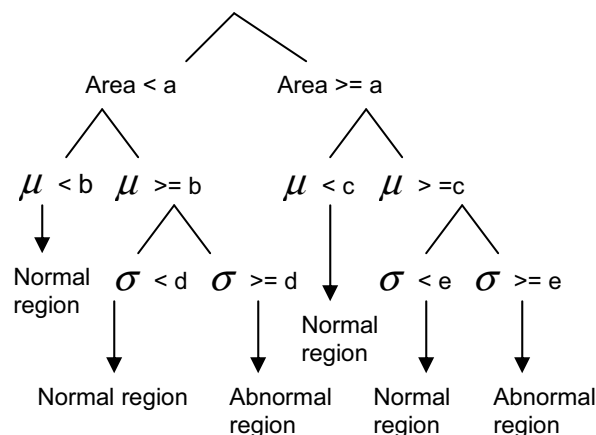


Fig. 7. Tree diagram for classification of the regions that not adjacent to skull. The notations  $\mu$ ,  $\sigma$ ,  $a$ ,  $b$ ,  $c$ ,  $d$  and  $e$  denote the mean, standard deviation, threshold value for the area, mean of the smaller area, mean of the larger area, standard deviation of the smaller area and standard deviation of the larger area respectively.

### 3.6 EM Segmentation

Eventually, we employ the EM to segment the intracranial area into two clusters which are CSF and brain matter. The EM algorithm (e.g., A. Dempster et al, 1977; Tong et al, 2008) is a widely used statistical estimation algorithm for finding maximum likelihood estimates of parameters in probabilistic models.

Using the EM segmentation allows each pixel to be assigned to a cluster and iterate to increase the overall likelihood. The procedure to segment the CSF and brain matter work as below:

- Find the initial values for the maximum likelihood parameters which are means, covariances and mixing weights.
- In expectation (E) step, use the probability density function for a Gaussian distribution to compute the cluster probability for every pixel. The multivariate Gaussian conditional density function is written as:

$$f_i(x|\theta_i) = \frac{1}{(2\pi)^{d/2} |\Sigma_i|^{1/2}} \exp\left[-\frac{1}{2}(x-\mu_i)^T \Sigma_i^{-1}(x-\mu_i)\right]$$

where  $\theta_i = (\mu_i, \Sigma_i)$ ,  $x$  is a  $d$ -dimensional feature vector,  $\mu_i$  is the mean vector and  $\Sigma_i$ ,  $|\Sigma_i|$  and  $\Sigma_i^{-1}$  are the  $d \times d$  covariance matrix, its determinant and inverse respectively.

- In the maximization (M) step, use the probability values obtained in E-step to re-compute the means, covariances and mixing weights. The goal is to select the parameters that minimize the deviation error weighted by the segmentation.
- Repeat E-step in (ii) and M-step in (iii).

The algorithm terminates when the difference between the log likelihood for the previous

iteration and current iteration fulfills the tolerance.

## 4. Experimental Results

### 4.1 EM Segmentation Results and Discussion

The CT head images used are provided by the collaborating hospital and the medical doctor has manually labeled regions in the brain. The dimension of the image is 512 x 512 and all the images are in DICOM format. The image depth is 16-bit-depth. For the images with the presence of abnormal regions, we experimented on 28 patients and for each patient we utilize 2 images. As a result, all the images contribute a total of 114 potential abnormal regions. We have tested our system on EM segmentation for two types of images which are the brain image with abnormal regions and without abnormal regions. The CT head image with abnormal regions is eventually categorized into three clusters which are CSF, brain matter and abnormal regions. However, for the images without abnormal regions, only two clusters exist which are CSF and brain matter cluster. The results of all the clusters are shown in Fig. 8.

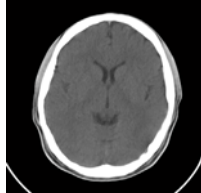
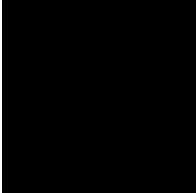


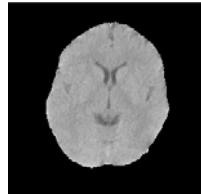



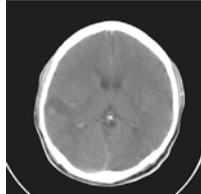
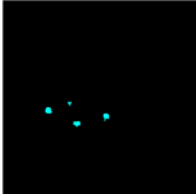
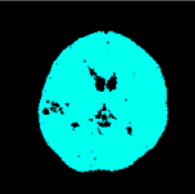
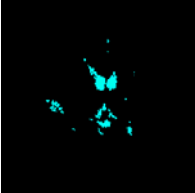
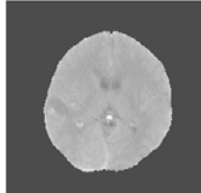

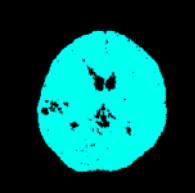
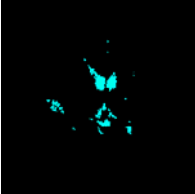


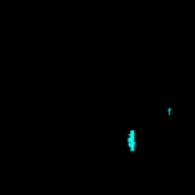

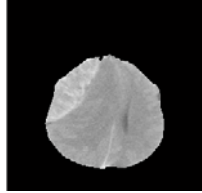
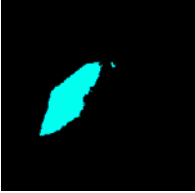
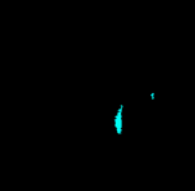

| No. | CT Head Image & Its Intracranial Area:  | Method: | Abnormal Regions:  | Brain Matter:   | CSF:  |
|-----|---|---------|--|---|---|
| 1:  |  | k-means |  |  |  |
|     |  | FCM     |  |  |  |
| 2:  |  | k-means |  |  |  |
|     |  | FCM     |  |  |  |
| 3:  |  | k-means |  |  |  |
|     |  | FCM     |  |  |  |

Fig. 8. The results of the segmentation of CT head images

For the images without the abnormal regions the image display under abnormal region's column will be left black as in the first example in Figure 8. From the obtained results, the combination of different methods for the head image segmentation is effectively workable on the acquired CT images.

#### 4.2 Classification Results and Discussion

We run our whole system on a computer with Intel Pentium-4 2.9GHz and 512MB main memory with average less than 45 seconds and 55 seconds for k-means clustering and FCM clustering respectively per image. We evaluated our results from Section 3.5 for the classification accuracy of the abnormal regions in terms of precision and recall. The comparison results for both k-means and FCM clustering are depicted in Table 2. In our classification, precision and recall are defined as follows:

$$\text{Precision} = \frac{\text{Numbers of abnormal regions correctly classified}}{\text{Total regions classified as abnormal regions}}$$

$$\text{Recall} = \frac{\text{Numbers of abnormal regions correctly classified}}{\text{Total abnormal regions}}$$

Table 2 Results of the classification of the abnormal regions

|         | Precision | Recall |
|---------|-----------|--------|
| k-means | 98.96%    | 83.33% |
| FCM     | 98.92%    | 80.70% |

For both k-means and FCM clustering, the percentage of the precision is higher due to only few normal regions are misclassified as abnormal regions. Whereas the result of recall is lower as for those misclassified as abnormal regions their intensity is very similar to the white matter of the brain even after we have done two contrast enhancements. However, the recall for k-means clustering is slightly better than FCM clustering as FCM clustering appears to be more sensitive to the noise. It has a tendency of including some surrounding noise pixels into the abnormal regions which cause the over-segmentation of the abnormal region. This reduces the benefits of the fuzzy classification. One of the examples for the over-segmentation we encountered is shown in Fig. 9. The over-segmentation reduces the average of pixels in the region and makes it misclassified as normal region. For those misclassified abnormal regions, they will be merged into the brain matter cluster in EM segmentation.

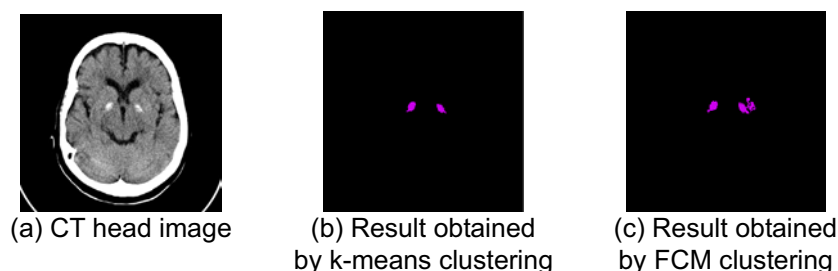


Fig. 9. Example of the comparison result between k-means and FCM clustering.

## 5. Conclusion

As a conclusion, we have presented our concept for the real CT head image segmentation. The system performs image segmentation based on different approaches for the different regions of the brain at different stages. The method works effectively for detection of the abnormal regions in the brain and general annotation of the abnormalities can be utilized for the retrieval application.

Plans for future work include the specific annotation of the abnormal regions such as hemorrhage, calcification and lesion and their effectiveness in image retrieval application.

### ***Acknowledgment***

The authors would like to express their gratitude to Dr. Fatimah Othman from Putrajaya Hospital for the images provided, support and consultation from time to time. Besides that, they would also like to express appreciation to MOSTI for funding support under grant #01-02-01-SF0014 to make this project possible.

### ***References***

- A. Dempster, N. Laird, and D. Rubin, "Maximum Likelihood from Incomplete Data via the EM Algorithm", *J. Royal Statistical Soc.*, vol. 39, 1977, pp. 1-38.
- Albert Huang, Rafeef Abugharbieh, Roger Tam, Anthony Trabousee, "MRI Brain Extraction with Combined Expectation Maximization and Geodesic Active Contours", *Signal Processing and Information Technology*, 2006 IEEE International Symposium, Aug. 2006, pp.107-111.
- Dubravko Covic, Sven Loncaric, "Rule-Based Labeling of CT Head Image", 6th Conference on Artificial Intelligence in Medicine, 1997, pp. 453-456
- K.H. Hohne and W.A. Hanson, "Interactive 3D segmentation of MRI and CT volumes using morphological operations", *J. Comp. Assist. Tomogr.* 2, 1992, pp. 285-294.
- Lemieux L., Hagemann G., Krakow K., Woermann F.G., "Fast, accurate, and reproducible automatic segmentation of the brain in T1-weighted volume MRI data", *Magnetic Resonance in Medicine* 42, 1999, pp.127-135.
- MATESIN Milan, LONCARIC Sven, PETRAVIC Damir, "A rule-based approach to stroke lesion analysis from CT brain images", 2nd international symposium on image and signal processing and analysis, June 2001, pp. 219-223
- N. A. Mohamed, M. N. Ahmed, and A. Farag, "Modified Fuzzy C-Mean in Medical Image Segmentation", *Acoustics, Speech, and Signal Proceedings*, vol.6, 1999, pp. 3429-3432.
- Nathalie Richarda, Michel Dojata, Catherine Garbayvol, "Distributed Markovian segmentation: Application to MR brain scans", *Journal of Pattern Recognition* 40, 2007, pp. 3467-3480.
- Qingmao Hu, Guoyu Qian, Aamer Aziz, Wieslaw L. Nowinski, "Segmentation of brain from computed tomography head images", *Proceedings of IEEE Engineering in Medicine and Biology 27<sup>th</sup> Annual conference*, Sept. 2005, pp. 3375 - 3378.
- Ruzica Maksimovic, Srdjan Stankovic and Dragorad Milovanovic, "Computed tomography image analyzer: 3D reconstruction and segmentation applying active contour models snakes", *International Journal of Medical Informatics Volumes 58-59*, Sept. 2000, pp. 29-37.
- Tong Hau Lee, Mohammad Faizal Ahmad Fauzi and Ryoichi Komiya, "Segmentation of CT Head Images", *Conference on Biomedical Engineering and Informatics*, 2008.
- Wei Kaiping, He Bin, Zhang Tao, Shen Xianjun, "A Novel Method for Segmentation of CT Head Images", *International Conference on Bioinformatics and Biomedical Engineering*, July 2007, pp. 717-720.
- Y. Zhang, M. Brady, S. Smith, "Segmentation of brain MR images through a hidden Markov random field model and the expectation-maximization algorithm", *IEEE Transactions Medical Imaging*, vol. 20, Jan. 2001, pp. 45-57.

### ***Author Profile***



Tong Hau Lee: He received his M.Sc. (IT) in 2001 from University Sains Malaysia. He works in Multimedia University as a lecturer since 2001. His research interest is in digital image processing such as image segmentation and semantics-based image retrieval.



Mohammad Faizal Ahmad Fauzi: He received the B.Eng. degree in electrical and electronic engineering from Imperial College, London, UK in 1999, and the Ph.D. degree in electronics and computer science from University of Southampton, Southampton, UK in 2004. He is currently attached to the Multimedia University, Malaysia as a lecturer/researcher. His main research interests are in the area of signal processing, analysis, retrieval and compression of image, audio and video data, as well as biometrics.



Ryoichi Komiya: He received the B.E. and Ph.D. degrees from Waseda University, Tokyo, Japan, in 1967 and 1986, respectively. Since 1998, he has been at Multimedia University Malaysia, where he has been responsible for research and development of next generation telecommunication systems, services, terminals, IP network, virtual education environment, e-commerce terminal and Intelligent Transportation System. From 2006 to 2008, he was at National Institute of Information and Communication Technology, Japan where he has been promoting R&D on medical ICT. He is currently a visiting professor at Faculty of Software and Information of Iwate Prefectural University, Japan.